

Photosynthesis, yield, energy balance, and water-use of intercropped maize and soybean

Elena A. Pelech¹  | Brendan C. S. Alexander²  | Carl J. Bernacchi^{3,1} 

¹Carl R Woese Institute for Genomic Biology, University of Illinois at Urbana-Champaign, Urbana, Illinois, USA

²Lethbridge Research and Development Centre, Agriculture and Agri-Food Canada, Lethbridge, Alberta, Canada

³USDA-ARS Global Change and Photosynthesis Research Unit, Urbana, Illinois, USA

Correspondence

Carl J. Bernacchi, 1201 W. Gregory Drive, Urbana, IL 61801 (217) 333-8048, USA.
Email: carl.bernacchi@usda.gov

Funding information

Global Change and Photosynthesis Research Unit of the USDA Agricultural Research Service

Abstract

By 2050, the U.S. Corn Belt will likely face a 23% increase in leaf-to-air vapor pressure deficit (VPD_L), the driving force of evapotranspiration (ET), which may restrict maize yield improvements for rainfed agroecosystems. Alternative cropping systems, such as maize and legume intercrops, have previously demonstrated yield and resource-use advantages over monocultures. In this study, the residual energy balance approach was used to gain insights into how an additive simultaneous maize and soybean intercrop system regulates ET and water-use efficiency (WUE) compared to standard maize and soybean monoculture systems of the U.S. Corn Belt. Experimental field plots were rain-fed and arranged in a randomized complete block design in three blocks. Photosynthetic capacity and grain yield of maize were conserved in the intercrop. However, its competitive dominance shaded 80%–90% of incident light for intercropped soybean at canopy closure, leading to a 94% decrease in grain yield compared to soybean monoculture. The total grain yield per unit area of the additive intercrop (land-use efficiency) increased by $11\% \pm 6\%$ (1 SE). Compared to maize monoculture, the intercrop had higher latent heat fluxes (λET) at night but lower daytime λET as the intercrop canopy surface temperature was approximately $.25^\circ\text{C}$ warmer, partitioning more energy to sensible heat flux. However, the diel differences in λET fluxes were not sufficient to establish a statistically significant or biologically relevant decrease in seasonal water-use (ΣET). Likewise, the increase in land-use efficiency by the intercrop was not sufficient to establish an increase in seasonal water-use efficiency. Intercropping high-performing maize and soybean cultivars in a dense configuration without negative impact suggests that efforts to increase yield and WUE may lead to improved benefits.

KEYWORDS

evapotranspiration, intercropping, photosynthetic capacity, water-use efficiency

1 | INTRODUCTION

Climate change poses important challenges to sustain food and bio-energy security for an increasing population (Tilman et al., 2011). Over

three decades, air temperature increases for the continental USA have driven higher vapor pressure deficits (Ficklin & Novick, 2017), the difference between the saturation vapor pressure of air and the actual vapor pressure. Specifically, the leaf-to-air vapor pressure deficit

 This is an open access article under the terms of the Creative Commons Attribution-NonCommercial License, which permits use, distribution and reproduction in any medium, provided the original work is properly cited and is not used for commercial purposes.

© 2021 The Authors. *Plant Direct* published by American Society of Plant Biologists and the Society for Experimental Biology and John Wiley & Sons Ltd. This article has been contributed to by US Government employees and their work is in the public domain in the USA.

(VPD_L) is the driving force of evapotranspiration (ET), consisting of up to three separate water vapor fluxes: evaporation of water from the soil and plant surfaces and the transpiration of water by plants. Climate models predict that by 2050, the Midwestern U.S. will face further increases in air temperature but fewer annual precipitation changes, which will propel a 23% increase in VPD_L (Lobell et al., 2009). Thus, the acceleration of ET may halt further maize yield gains for rainfed agroecosystems within the Midwestern U.S. Corn Belt (DeLucia et al., 2019; Ort & Long, 2014). Opportunities to improve water-use efficiency (WUE) are consequently critical.

Intercropping is the simultaneous or relay cultivation of multiple crops on the same field during a significant part of their growth cycle which aims to match, or potentially exceed, crop productivity of standard monoculture systems (Li et al., 2020; Vandermeer, 1989). Advantages of intercrops emerge from higher resource utilization, such as solar radiation, water, and nutrients by beneficial neighbor interactions (facilitation and niche complementarity) or by the dominance of a very productive crop species or genotype (selection) (Brooker et al., 2015; Cardinale et al., 2007). Thus, intercropping systems can increase productivity per unit of land area and WUE if optimally managed. Efforts to gain a mechanistic understanding of how such advantages may be realized will likely aid the adoption of such practices. The energy balance approach was used in this study to gain insights on how an additive alternate-row intercrop system of maize and soybean sowed simultaneously regulates ET and WUE.

Plant canopies play a crucial role in regulating the partitioning of available energy (net radiation) to sensible (convection and conduction) and latent (evaporation of water) heat fluxes, with a small fraction of energy driving net leaf photosynthetic carbon assimilation (Bernacchi & VanLoocke, 2014). Under dynamic control of the plant, stomatal conductance determines the ease of CO₂ uptake for photosynthesis and the flux of water vapor to the bulk atmosphere by the process of transpiration (Lawson & Blatt, 2014), which is the dominant flux contributing to ET when CO₂ uptake is the strongest (Bernacchi et al., 2007). The physical environment within plant canopies also affects water vapor movement from leaves to the bulk atmosphere. Plant canopy architecture determines leaf and canopy boundary layers which feedback on wind speed, surface roughness, and atmospheric stability; essential factors contributing to ecosystem fluxes (Bernacchi & VanLoocke, 2014).

Intercrop canopies inherently have more complexity within the system's physiological and structural dimensions than monocultures, where the partitioning of energy to sensible and latent heat fluxes may be considerably different. Specifically, the release of water vapor within an intercrop canopy composed of two crops differing in stature and growth dynamics may reduce the VPD_L within the understory. The structural dominance of tall maize creates shade and windbreak conditions in the vicinity of shorter soybean reducing VPD_L within the microclimate (Morris & Garrity, 1993). In response, stomatal conductance of soybean may increase, transpiring more water vapor from the soil to the air. However, competition for water may arise between maize and soybean, especially for additive and simultaneous intercrop designs (Arshad, 2021; Arshad et al., 2020). Therefore, stomatal conductance may decrease for both crops when soil water becomes

limiting, and a greater amount of energy will be partitioned to sensible heat fluxes away from the canopy than latent heat fluxes (Bernacchi & VanLoocke, 2014). Gains in WUE may be realized if the intercrop productivity maintains or exceeds the performance of the individual crop in monoculture. On the other hand, competition for light and water between maize and soybean in proximity may decrease total yield and offset any increases in WUE.

Light interception, leaf photosynthetic capacity, and seasonal ET were measured for a simultaneous and additive alternate-row intercropping system (Figure 1) which was compared to the standard maize and soybean monocultures of the U.S. Corn Belt under rain-fed conditions to assess the potential for a polyculture system to improve WUE. The plant density of each component crop in the intercrop was equal to their respective monoculture. We hypothesized that the added complexity within the physiological and structural dimensions of an additive and simultaneous maize/soybean intercrop canopy will maintain grain yield per unit land area but lead to a decrease in seasonal ET and consequently increase WUE compared to the standard monoculture systems of the U.S. Corn Belt. The results will provide insight into how the added spatial complexity in an intercropping system regulates the biophysical factors that influence water-use.

2 | METHODS

2.1 | Site description

The rainfed field experiment was situated at the Energy Farm at the University of Illinois, Urbana-Champaign (40°03'N, 88°12', 215 m above sea level) during the 2018 growing season. The site previously maintained a 2-year rotation of maize and soybean, where no nitrogen fertilizer was added before or after soybean planting, which is in accordance with the standard regional practice. Soils at the experimental site are Drummer silty clay loam that is deep and poorly drained (Soil Survey Staff, 2015). Before planting, 202 kg N ha⁻¹ as urea granules (ESN, Smart Nitrogen) was applied by hand across the experimental area. Daily meteorological data over the growing season from planting to harvest were obtained from the mean of three weather stations on site (Figure 2).

Experimental plots were arranged in a completely randomized block design with three replicates for each cropping system to account for topographic and soil variation across the field. Hybrid maize (*Zea mays* L. [DEKALB DKC63-60RIB]) and indeterminate soybean (*Glycine max* L. Merr. [Asgrow AG36X6]) were sown simultaneously on May 24 under both monoculture and intercrop systems with a 6-row seed drill planter. All experimental plots consisted of 3 m rows running north-south and were harvested at physiological maturity on September 27 (119 days after emergence [DAE]). The monoculture plots consisted of two cropping systems; (i) 6 maize rows with a row spacing of .76 m at a planting density of 8.4 plants m⁻² (M_{maize}); (ii) 6 soybean rows with a row spacing of .76 m at a planting density of 34.6 plants m⁻² (M_{soybean}). The intercropped plots (I_{maize/soybean}) consisted of 11 alternating rows of maize and soybean at .38 m row spacing and at equal planting densities as their respective

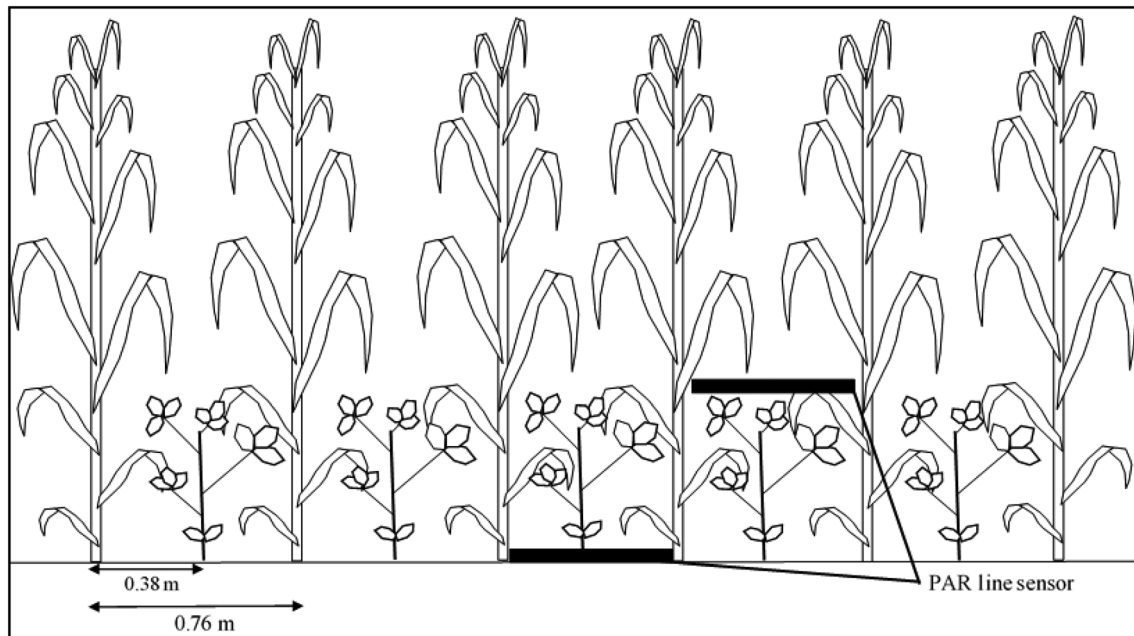


FIGURE 1 Illustrative representation of the intercrop system and sensor placement. A single row of soybean was sown between .76 m maize rows resulting in 11 alternating rows. The plant density of each species in the intercrop was equal to its respective monoculture, but collectively, the intercrop had a higher plant density than each monoculture (additive design). Rectangular bars indicate the placement of photosynthetically active radiation (PAR) line quantum sensors. A total of 2 sensors for each position were placed at a diagonal angle within the rows for greater spatial representation. The figure is not to scale

monocultures (Figure 1). Explicitly, the intercrop holds an additive design compared to both maize and soybean monocultures.

2.2 | Leaf gas exchange

All leaf-level gas exchange measurements with pulse amplitude modulated chlorophyll fluorescence were conducted with an open-path gas exchange system (LI6400XT, LI-COR, Lincoln, Nebraska, USA) equipped with a leaf chamber fluorometer of 2 cm². Measurements were conducted at two developmental stages for maize and soybean (vegetative V10 and blister R2, vegetative V5 and full pod R4, respectively [28 DAE and 63 DAE]). Two of the youngest fully expanded leaves were sampled predawn in each plot. The soybean petiole and maize leaf blade were then re-cut underwater and kept under low light until measurement in the laboratory. This procedure avoided transient decreases in water potential and maximum photosystem II efficiency, which can occur after dawn and alter photosynthetic responses.

Photosynthetic light response (A/Q) curves for maize and soybean consisted of 14 points from 2000 to 15 $\mu\text{mol m}^{-2} \text{s}^{-1}$ photosynthetic photon flux density (PPFD) following acclimation in 2000 $\mu\text{mol m}^{-2} \text{s}^{-1}$ PPFD. Measurement chamber conditions were set to 60%–80% humidity, a block temperature of 23°C, and 410 ppm reference CO₂ concentration in the airstream. When a steady state was reached (minimum of 2 min at each light level), gas exchange parameters were logged with light-adapted steady-state fluorescence (F_s), minimal fluorescence (F_o'), and maximal fluorescence (F_m') to estimate the

operating efficiency of photosystem II (ϕ_{PSII}) as $(F_m' - F_s)/F_m'$ (Baker, 2008). Photosynthetic CO₂ response (A/C_i) curves for maize and soybean consisted of 10 CO₂ concentrations in the sequence: 410, 300, 200, 100, 50, 410, 410, 600, 800, and 1000 ppm. Humidity and block temperature were set as described for A/Q curves above, except that PPFD was set to 2000 and 1800 $\mu\text{mol m}^{-2} \text{s}^{-1}$ for maize and soybean, respectively.

For soybean, the maximum carboxylation rate of Rubisco ($V_{c,max}$) and the maximum rate of electron transport (J_{max}) were determined according to Long and Bernacchi (2003). The soybean A/Q curves and all maize response curves were fitted to the models described by Bellasio et al. (2015) and Bellasio et al. (2016) to derive: light-saturated CO₂ assimilation (A_{sat}), the apparent quantum yield of CO₂ assimilation (AQY), light compensation point (LCP), dark respiration rate (R_d), the quantum yield of photosystem II (ϕ_{PSII}), C_i – A compensation point (Γ), stomatal limitation (l) and, CO₂-saturated phosphoenolpyruvate carboxylase (PEPC) carboxylation rate ($V_{p,max}$).

2.3 | Micrometeorological measurements

A residual energy balance approach was used to determine evapotranspiration (ET) from individual plots according to

$$\lambda ET = R_n - G_0 - H \quad (1)$$

where λ was the latent heat of vaporization (2,256,000 J kg⁻¹), ET was evapotranspiration (kg m⁻² s⁻¹; positive upward), R_n was net radiation

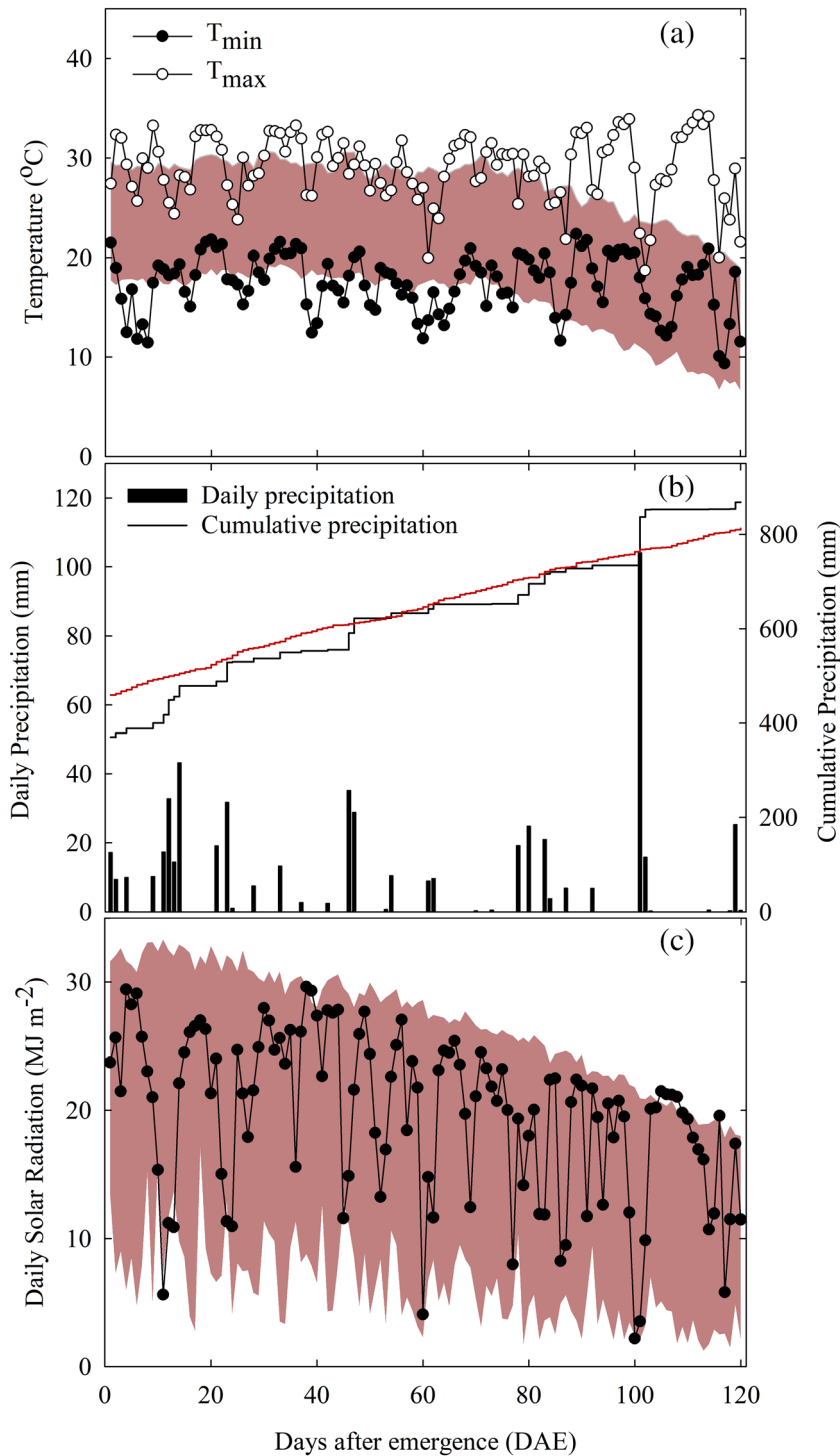


FIGURE 2 Daily meteorological observations for the 2018 growing season. (a) Maximum (white circle) and minimum (black circle) daily mean temperatures which overlay 30-year mean temperature ranges (red band); (b) daily (black bar) and cumulative (black line) precipitation with the cumulative 30-year mean precipitation (red line); and (c) daily incident solar radiation (black circle) which overlays the 30-year mean range (red band). Precipitation and incident solar radiation data were collected from three onsite weather stations, and temperature data were collected over experimental plots. Historical weather data were obtained from the Illinois Climate Network (<https://doi.org/10.13012/J8MW2F2Q>)

($W m^{-2}$; positive downward), G_0 was soil surface heat flux ($W m^{-2}$; positive downward), and H was sensible heat flux ($W m^{-2}$; positive downward) (Bernacchi et al., 2007; Jackson et al., 1987; Kimball et al., 1999; Triggs et al., 2004). This approach depends on four energy fluxes into and out of canopies and ignores energy fluxes due to photosynthesis, respiration, and heat storage within a canopy over a 24-h period, which is less than 1% of incoming radiation (Meyers & Hollinger, 2004). While the residual energy balance approach does not measure ET directly, it has proven to be useful in obtaining

quantitative estimates of ET (e.g., Bernacchi et al., 2007). Other meteorological methods that directly measure ET, such as eddy covariance and flux gradient analysis (Baldocchi et al., 1988), require a greater experimental area and affluent resources.

A micrometeorological station was situated between plots equipped and connected to sensors in each plot to measure each of the three energy flux parameters on the right side of Equation (1). All R_n , G_0 , and H measurements were logged at 30-s intervals and averaged over 30 min using a data logger (model CR1000 with AM16/32B

multiplexer, Campbell Scientific, Logan, UT, USA). The station was operated with online power with a battery backup to minimize downtime in a power outage. The datalogger stored and transmitted measurements to a central computer via radio. Data were checked daily for errors, and instruments were inspected and cleaned weekly.

Data collection began at canopy closure (47 DAE) and ended just prior to senescence (99 DAE), totalling 52 measurement days. The period before canopy closure is disproportionately affected by the dark soils found throughout the Midwestern U.S. and results in high H and G_0 for those days. The diurnal trends for G_0 did not follow the expected sigmoidal increases and decreases at canopy closure, suggesting that the data were inaccurate and were omitted from the equation. Soil heat flux is meaningful but integrated over a whole day or season represents a very small fraction of the total cumulative energy flux and thus, the influence of G_0 on ET is negligible.

2.4 | Net radiation, R_n

Net radiation (R_n ; $W m^{-2}$) is equal to the sum of net shortwave (R_{NETSW} ; $W m^{-2}$) and net longwave (R_{NETLW} ; $W m^{-2}$) radiation,

$$R_n = R_{NETSW} + R_{NETLW} \quad (2)$$

Measurements were collected using two-channel net radiometers (model CRN2, Kipp and Zonen, Delft, The Netherlands), where one sensor was placed in a single replicate of each monoculture plot, and two sensors were placed in a single replicate of an intercrop plot above each species. Two pyranometers measured the shortwave radiation, and two pyrgeometers measured the longwave radiation, incoming from the sky and reflected from the canopy surface, respectively. Net radiometers were placed 1 m above the canopy surface and were raised as the canopy grew. Factory calibration of the sensors was conducted before the growing season.

2.5 | Sensible heat flux, H

Sensible heat flux (H ; $W m^{-2}$) was calculated as,

$$H = \rho_a c_p \frac{T_s - T_a}{r_a} \quad (3)$$

where ρ_a was air density ($kg m^{-3}$), c_p was heat capacity of air ($1020 J kg^{-1} C^{-1}$), T_s was the surface temperature ($^{\circ}C$), T_a was air temperature ($^{\circ}C$), and r_a was aerodynamic resistance ($s m^{-1}$). Calculation of r_a was determined by the previously described model, which can be found in the supporting information S1 (Jackson et al., 1987). The aerodynamic resistance model relies on wind speed measured using a 2-axis ultrasonic anemometer (model 85,000 R.M. Young Company, Traverse City, MI, USA) and canopy height, measured weekly throughout the season. Air temperature and humidity were measured using an HMP60-L temperature and humidity probe

(Campbell Scientific, Logan, UT, USA) installed in a solar radiation shield (model 41003, R. M. Young, Traverse City, MI, USA), which reflects solar radiation to keep the probe near ambient temperature. Surface temperatures were measured using infrared thermometers where a single sensor was placed in each monoculture plot, and two sensors were placed in each intercrop plot (model IRT-P, Apogee Instruments, Logan, UT, USA).

2.6 | Water-use, ΣET and water-use efficiency

The relationship between latent heat flux (λET) and ET is that λET is the amount of energy ($W m^{-2}$) consumed when evaporating a quantity of water over time. The latent heat of vaporization was used to convert energy to mass volume. To get values of ET in units of mm season, integration of ET $mm s^{-1}$ concerning time over the growing season was calculated using midpoint Riemann sums where n is the number of ET measurements over the season,

$$\Sigma ET = \sum_i^n ET_i \times 1800s \quad (4)$$

Integrated water-use efficiency (WUE) was then calculated according to Condon et al., 2002 and Bernacchi & VanLoocke, 2014,

$$WUE = \frac{yield (gm^{-2})}{\Sigma ET} \quad (5)$$

2.7 | Light interception

Daily canopy light interception fractions and seasonal interception efficiency (ϵ_i) were calculated as

$$\epsilon_i = 1 - \left(\frac{I_t + I_r}{I_o} \right) \quad (6)$$

where I_o was incident photosynthetic photon flux density (PPFD $\mu mol m^{-2} s^{-1}$) measured using a downwelling quantum sensor (LI-190, LI-COR, Lincoln, NE, USA) from an onsite weather station, I_t was transmitted PPFD ($\mu mol m^{-2} s^{-1}$) measured at .1 m from the soil surface using two line quantum sensors (model SQ-311, Apogee Instruments, Logan, UT, USA) and I_r was reflected PPFD ($\mu mol m^{-2} s^{-1}$) using the net radiometers 1 m above the canopy assuming no reflected radiation from the soil surface. In addition, two line quantum sensors were placed .5 m above the intercropped soybean to measure PPFD ($\mu mol m^{-2} s^{-1}$) above soybean plants and between maize rows.

All quantum line sensors were calibrated before and after the experiment against a factory calibrated sensor over three clear days. All data between canopy closure (47 DAE) and prior to senescence (99 DAE) were logged every 30 s and averaged over 30-min intervals using the same data logger connected to the sensors to calculate ET (model CR1000 with AM16/32B multiplexer, Campbell Scientific,

Logan, UT, USA). All quantum sensors were cleaned and adjusted in height to maintain their constant distances from the growing canopy surface every week. Data were checked for errors daily.

2.8 | Leaf area index; LAI

A leaf canopy analyzer (LAI-2200, LI-COR, Lincoln, NE, USA) was used to measure LAI every week around solar noon on clear sunny days. Two rows were measured with four below canopy readings coupled with one reading above the canopy for the monoculture plots. To account for the greater spatial heterogeneity within the intercrop canopy, six below canopy readings parallel and perpendicular to the crop rows coupled with one reading above the canopy. A lens cover was used to permit a 90° field of view for all measurements.

2.9 | Grain yield and land-use efficiency

The grain yield response of maize and soybean was collected at physiological maturity (119 DAE), where two 1 m samples per plot were harvested from the center rows by hand. Pods and cobs were stored in a drying oven at 60°C for 6 days before threshing and weighing. The land equivalent ratio (LER, Vandermeer, 1989) was used to assess land-use efficiency of the intercrop calculated as

$$\text{LER} = \frac{Y_{\text{I maize}}}{Y_{\text{M maize}}} + \frac{Y_{\text{I soybean}}}{Y_{\text{M soybean}}} \quad (7)$$

where $Y_{\text{I maize}}$ and $Y_{\text{I soybean}}$ are the yields (g m^{-2}) of maize and soybean in the intercrop system, respectively, and $Y_{\text{M maize}}$ and $Y_{\text{M soybean}}$ are the yields (g m^{-2}) of maize and soybean in the monoculture system, respectively. If $\text{LER} > 1$, the intercrop system has a yield advantage and increased land-use per unit area.

2.10 | Data and statistical analysis

Statistical analysis was performed using R software (R Core Team, 2021). Analysis of variance (ANOVA) was carried out using the lme function (package “nlme,” Pinheiro et al., 2021) with cropping system and time-point considered fixed effects and block and block by replicate plot effects considered random. Plot mean A_{sat} , AQY, LCP, R_d , ϕPSII , Γ^* , I , V_p , max , V_c , max , J , max , and LAI were analyzed as repeated measures with growth stage/days after emergence (GS/DAE) as the repeated time-point factor (fixed effect). Diel energy fluxes and canopy surface temperature were also analyzed as repeated measures with time of day (TOD) as the repeated time-point factor, and to account for the heterogeneous diel variances, the model allowed unequal variance per TOD and cropping system, as well as an AR(1) correlation structure. Given the inherently

different functional and structural characteristics of the M_{soybean} canopy compared to those involving maize, diel flux comparisons with M_{soybean} were omitted. The average diurnal course of the absolute differences between the maize monoculture and alternate-row intercrop were also analyzed as repeated measures with TOD as the repeated time-point factor with unequal variance per TOD and cropping system as well as an AR(1) correlation structure. Statistical analyses on ϵ_i , ΣET and WUE were conducted using plot means, while yield analyses were separated by species, log-transformed, and conducted using plot subsamples ($n = 3$, 2 subsamples per plot, 6 total observations per treatment). Multiple pairwise comparisons between cropping system treatments were conducted using the emmeans function and Tukey's HSD was used to control 3 pairwise comparisons for ΣET and WUE (package “emmeans,” Lenth, 2021). The residuals were graphically checked for normality (qqplots) and constant variance (standardized residuals vs. fitted values), and an α of .1 was used to determine statistical significance to reduce the probability of type II errors.

3 | RESULTS

3.1 | Meteorological conditions during the 2018 growing season

Most daily maximum temperatures were higher than the seasonal 30-year mean temperature ranges (Figure 2a). Cumulative precipitation rates across the growing season were similar to the cumulative 30-year mean precipitation rates, excluding 100 DAE, when there was approximately 100 mm of precipitation (Figure 2b). Daily solar radiation values fell within the 30-year mean range (Figure 2c).

The arrangement of maize rows running north–south shaded 80%–90% of incident light to intercropped soybean (I_{soybean} , Figure 3). Therefore, the simultaneous alternate-row intercrop system provided 10%–20% of incident light for intercropped soybean between canopy closure and prior senescence.

3.2 | The intercropping system had the highest LAI and, consequently, the greatest ϵ_i

A statistically significant interaction between days after emergence (DAE) by cropping system and LAI was found where differences became apparent on 27 DAE (Table S.1 and Figure 4a). The intercropping system ($I_{\text{maize/soybean}}$) had a higher LAI than monoculture soybean (M_{soybean}) during exponential growth ($p < .1$) before both systems reached maximum LAI between 5 and 6 ($p > .1$). The LAI of $I_{\text{maize/soybean}}$ was similar to monoculture maize (M_{maize}) during exponential growth ($p > .1$) before M_{maize} reached a lower maximum LAI of 4 at canopy closure ($p < .1$). Consequently, the seasonal light interception efficiency (ϵ_i) for $I_{\text{maize/soybean}}$ was higher than M_{maize} by 8% ($p < .1$; Figure 4b).

FIGURE 3 Photosynthetic photon flux density (PPFD) above maize and above intercropped soybean. During sunlight hours (07:00–18:00), mean PPFD for incident (black circles) and above intercropped soybean (above I_{soybean} , white circles) between .76 m maize rows in the alternate-row intercrop are indicated. Each point represents a 30-min interval of the day averaged across 52 days and two line quantum sensors per plot. Error bars represent ± 1 SE of the mean and $n = 3$ for all data points. Rows were north–south orientation

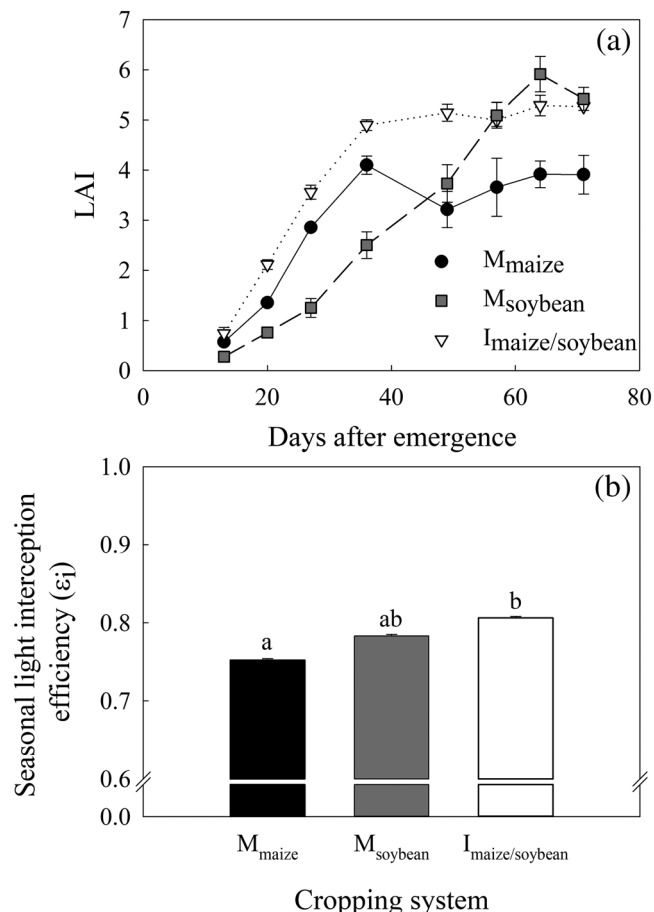
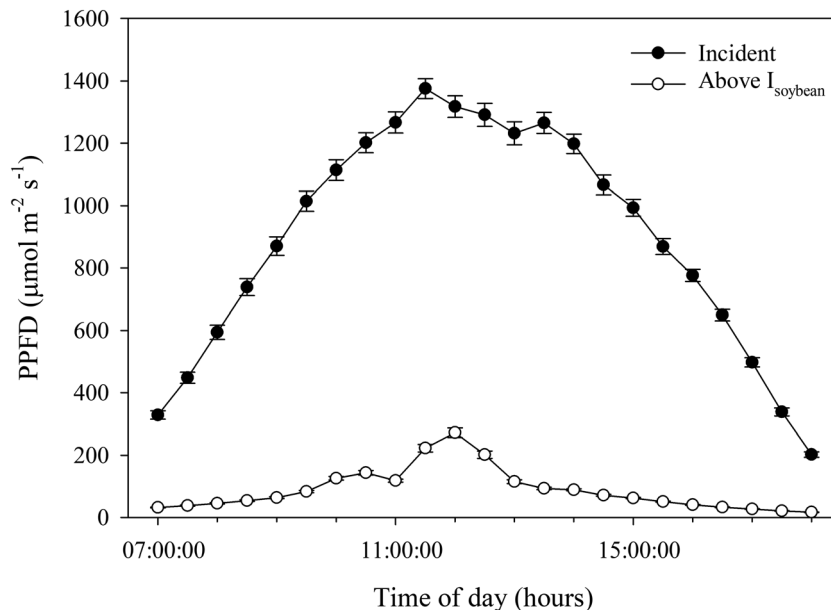


FIGURE 4 Leaf area index (LAI) and seasonal light interception efficiency (ϵ_i) across cropping systems. Mean LAI (a) for maize monoculture (white circles), soybean monoculture (gray circles), and alternate-row maize and soybean intercrop (black circles) across the season, and (b) mean ϵ_i across 52 measurement days for the same cropping systems where letters indicate significant differences ($\alpha = 0.1$). Error bars and replicates are as in Figure 3

3.3 | Intercropping decreased the photosynthetic capacity of soybean but not maize

Gas exchange measurements were conducted twice over the growing season encompassing vegetative and reproductive growth stages. Parameters derived from gas exchange measurements were analyzed individually at each growth stage (Table 1) and as a seasonal average (Figures 5 and 6). On individual sampling days and seasonally, intercropping did not affect the photosynthetic CO_2 and light response parameters of maize (Table 1, Figure 6, and Table S.1).

At vegetative growth (V5), those parameters related to the photosynthetic light response, excluding AQY, and $V_{c,\text{max}}$ were lower for I_{soybean} compared to M_{soybean} ($p < .1$, Table 1). At reproductive stage full pod (R4), decreases were observed for I_{soybean} photosynthetic CO_2 and light response parameters compared to M_{soybean} ($p < .1$), except for AQY, ϕPSII , Γ and I which were not affected by intercropping ($p > .1$, Table 1). Seasonally, the largest decreases for I_{soybean} were the parameters associated with the photosynthetic light response, with an 87% decrease in LCP, an 81% decrease in R_d , and a 44% decrease in A_{sat} ($p < .1$, Figure 5). Those parameters associated with biochemical capacity decreased by 36% for $V_{c,\text{max}}$, and 34% for J_{max} ($p < .1$, Figure 5).

3.4 | Responses of cropping system λET varied according to daily meteorological conditions

The residual energy balance approach to assess cropping system latent heat flux (λET) is heavily dependent on accurate measurements of canopy surface temperature (T_{canopy}) at canopy closure to determine sensible heat flux (H). Measured energy fluxes were averaged in 30-min intervals for all replicate plots, excluding net radiation measurements (R_n) since net radiometers were not replicated across plots.



TABLE 1 Parameters from photosynthetic light and CO₂ response curves at two growth stages for maize and soybean in monoculture (M) and intercrop (I)

Parameter	Maize				Soybean			
	Vegetative (V8)		Blister (R2)		Vegetative (V5)		Full pod (R4)	
	M	I	M	I	M	I	M	I
A_{sat}	50.09 ± 2.38	50.24 ± 2.64	40.68 ± .33	43.31 ± 4.05	26.86 ± .96	18.82* ± 2.64	34.61 ± .34	15.78* ± .40
AQY	.05 ± .01	.06 ± .01	.07 ± .01	.06 ± .01	.05 ± .01	.05 ± .01	.07 ± .01	.07 ± .01
LCP	54.22 ± 5.38	53.79 ± 4.08	35.42 ± 2.80	26.45 ± .97	33.87 ± 5.58	12.85* ± 2.34	27.55 ± .78	-5.04* ± 2.06
R_d	2.83 ± 0.21	2.96 ± .32	2.29 ± .19	1.65 ± 0.10	1.81 ± .16	.75* ± 0.11	1.89 ± .06	-.03* ± 0.11
$V_{c,\text{max}}$	—	—	—	—	95.94 ± 3.66	72.15* ± 7.14	110.10 ± 7.88	60.62* ± 1.83
$V_{p,\text{max}}$	133.67 ± 22.35	119.12 ± 13.95	77.10 ± 8.18	81.51 ± 3.48	—	—	—	—
J_{max}	—	—	—	—	151.64 ± 9.48	117.52 ± 10.09	176.47 ± 12.23	98.21* ± 4.96
ϕPSII	.64 ± .01	.66 ± .02	.70 ± .01	.70 ± .01	.67 ± .03	.64 ± .03	.74 ± .01	.67 ± .01
Γ	4.33 ± .76	3.66 ± .48	3.46 ± 1.05	4.19 ± .37	52.61 ± 1.31	56.49 ± .09	54.32 ± 1.51	58.47 ± 2.04
I	.07 ± .04	.07 ± .04	.14 ± .03	.14 ± .02	.06 ± .02	.06 ± .02	0.11 ± .02	0.10 ± .02

Note: Values represent the mean (±SE) of three replicate blocks ($n = 3$) with two subsamples. Significant differences compared to M are indicated with an asterisk at $\alpha = 0.1$.

An overcast ($R_n < 250 \text{ W m}^{-2}$, Figure 7b) and sunny day ($R_n > 500 \text{ W m}^{-2}$, Figure 7b) from the growing season at canopy closure are given as examples of energy flux, where λET is the amount of energy (W m^{-2}) consumed when evaporating a quantity of water over time, in this case, evapotranspiration (ET, Figure 7). The overcast and sunny days showed significant cropping system effects and time of day interactions for T_{canopy} , H , and λET (Figure 7 and Table S2). The dynamics of energy flux and canopy temperature over the overcast day were of smaller magnitude than the sunny day where T_{canopy} and H were lower for M_{soybean} than $I_{\text{maize/soybean}}$ around solar noon and λET was lower for M_{soybean} than M_{maize} (Figure 7 E-H, Table S2).

3.5 | Energy flux and canopy temperature were similar for the intercrop and maize monoculture

The intercrop T_{canopy} was approximately .25°C warmer than M_{maize} around solar noon, and at night, the intercrop T_{canopy} was modestly warmer (Figure 8a). However, T_{canopy} was only significantly affected by the time of day (Table S2). Intercropping showed diel differences of R_n , which was influenced by increases in longwave R_n during the day and night hours and increases in shortwave R_n between 8:00 and 13:00 before a decrease between 13:00 and 18:00 (Figure 8b). These oscillations were relatively small, the most considerable absolute difference between $I_{\text{maize/soybean}}$ and M_{maize} was 15 W m^{-2} , and maximum midday values were over 600 W m^{-2} (Figure 7f). Moreover, net radiometers were not replicated across blocks for statistical analysis. For H , the largest difference was around solar noon by approximately 16 W m^{-2} (Figure 8c); however, no significant differences were found for diel H between $I_{\text{maize/soybean}}$ and M_{maize} (Table S2).

The two measured energy fluxes, R_n , and H were used to calculate λET as the residual of the energy balance equation, and λET showed a significant cropping system effect and time of day interaction ($p < .1$, Table S2). The intercrop demonstrated significantly higher λET fluxes at night hours, but significantly lower λET fluxes during the day compared to M_{maize} (Figure 8d).

3.6 | ΣET and grain yield suggest no differences in water-use efficiency between maize systems

Integrated λET from 52 measurement days with over 5000 individual measurements of energy flux across the season showed that there were no significant differences in ΣET (mm season^{-1}) between $I_{\text{maize/soybean}}$ and M_{maize} ($p = .97$, Table 2). Only ΣET of M_{soybean} was higher than $I_{\text{maize/soybean}}$ and M_{maize} cropping systems ($p < .1$, Table 2).

There tended to be a 105% increase in maize yield in the intercrop at equal plant density ($p = .50$, Table 3), and intercropped soybean produced 6% of the grain yield in M_{soybean} at equal plant density ($p < .1$, Table 3). An LER of $1.11 \pm .06$ resulted (Table 3). Grain yield per unit ΣET , defined as water-use efficiency (WUE), was the greatest for $I_{\text{maize/soybean}}$ and the least for M_{soybean} (Table 2). However, at $\alpha = .1$, there was no statistically significant difference between WUE

FIGURE 5 Seasonal per cent change of gas exchange parameters for intercropped soybean compared to monoculture soybean. Light-saturated CO₂ assimilation (A_{sat}), the apparent quantum yield of CO₂ assimilation (AQY), light compensation point (LCP), dark respiration rate (R_d), the quantum yield of photosystem II (ϕ PSII), maximum rubisco carboxylation rate normalized to 25°C ($V_{c,max}$), the maximum rate of electron transport normalized to 25°C (J_{max}), C_i - A compensation point (Γ) and, stomatal limitation (l) are represented (\pm 95% CI, $n = 6$). Asterisks indicate that the per cent change in intercropping is significantly different from the monoculture system ($\alpha = 0.1$)

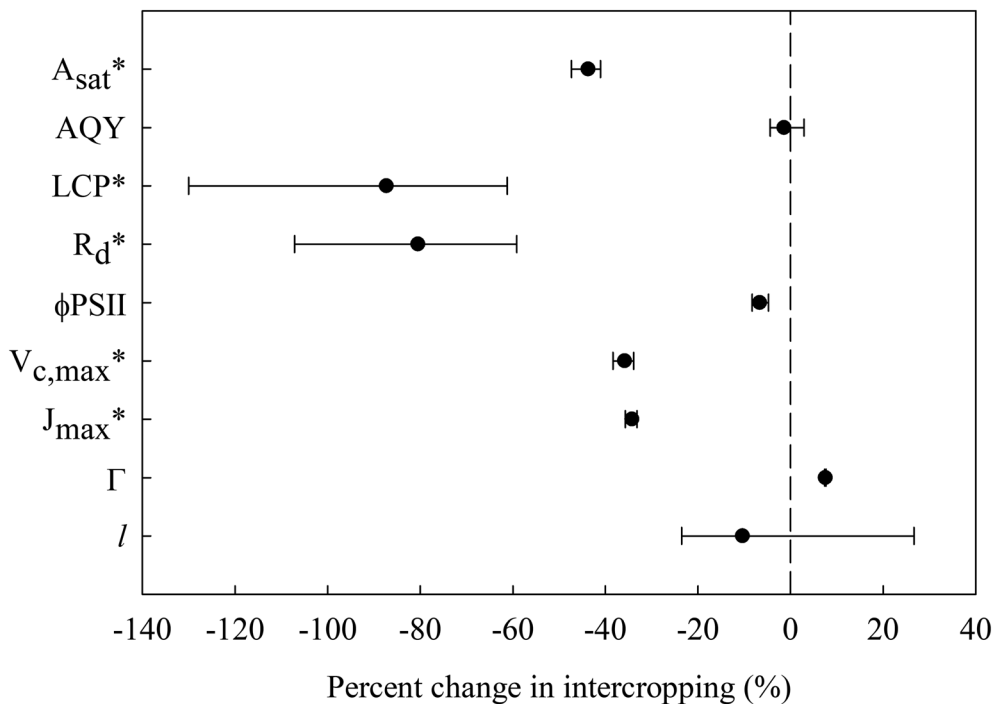
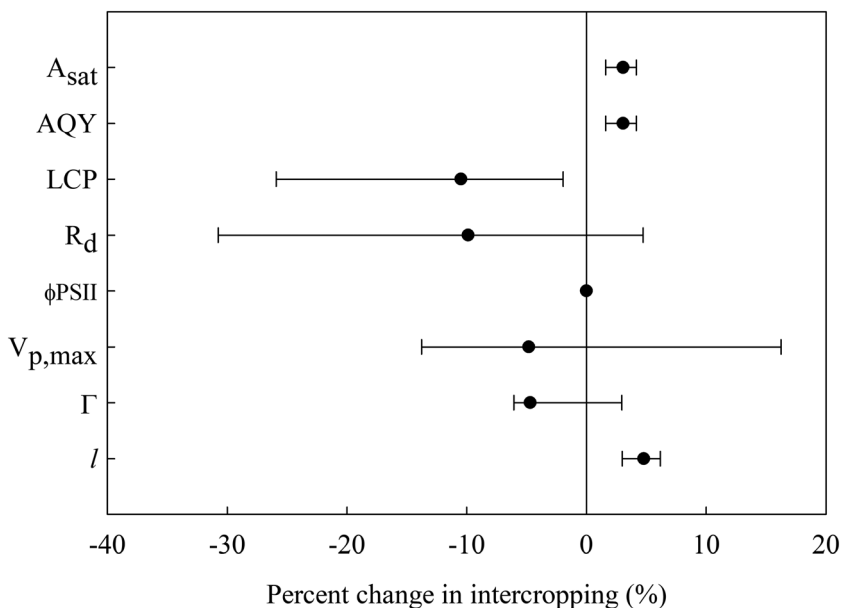


FIGURE 6 Seasonal per cent change of gas exchange parameters for intercropped maize compared to monoculture maize. Light-saturated CO₂ assimilation (A_{sat}), the apparent quantum yield of CO₂ assimilation (AQY), light compensation point (LCP), dark respiration rate (R_d), the quantum yield of photosystem II (ϕ PSII), CO₂-saturated phosphoenolpyruvate carboxylase (PEPC) carboxylation rate ($V_{p,max}$), C_i - A compensation point (Γ), and stomatal limitation (l) are represented (\pm 95% CI, $n = 6$). No significant differences were found



of the intercrop and monoculture maize ($p = .63$), only WUE of $M_{soybean}$ was significantly different than the $= I_{maize/soybean}$ and M_{maize} cropping systems ($p < .1$, Table 2).

4 | DISCUSSION

We hypothesized that the added complexity within the physiological and structural dimensions of an additive and simultaneous maize/soybean intercropping system with alternating rows would increase WUE compared to the standard monoculture systems of the

U.S. Corn Belt. This study found that LAI at canopy closure and ϵ_i for the intercrop was higher than the maize monoculture. Photosynthetic performance of intercropped maize was similar to monoculture maize, but intercropped soybean was substantially lower than monoculture soybean. Consequently, the intercrop decreased soybean grain yield while maize grain yield was conserved, and an LER of $1.11 \pm .06$ was achieved suggesting $11\% \pm 6\%$ more land area is needed for the standard monoculture systems to achieve the same yields as the additive and simultaneous intercrop. However, the residual energy balance approach revealed that the difference in seasonal water-use between the intercrop and maize monoculture was not statistically significant

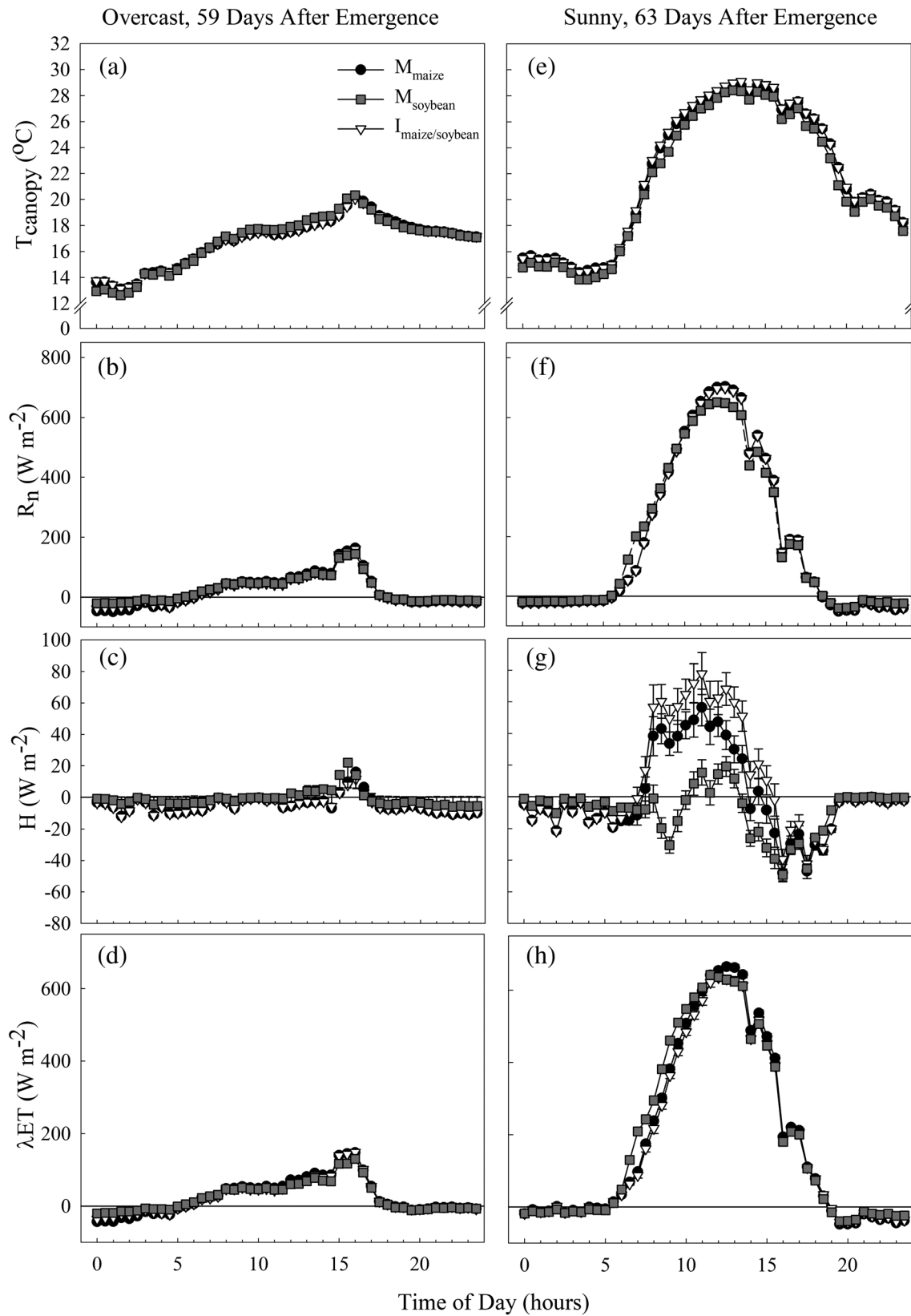


FIGURE 7 Energy flux over an example overcast and sunny day. Canopy surface temperature (T_{canopy}) (a and e), net radiation (R_n) (b and f), sensible heat flux (H) (c and g), and evapotranspiration (λET) (d and h) for monoculture maize (M_{maize} , black circle), monoculture soybean (M_{soybean} , dark gray square), and alternate-row maize and soybean intercrop ($I_{\text{maize/soybean}}$, white triangle) are represented. Error bars and replicates are as in Figure 3, excluding R_n , which was not replicated among blocks

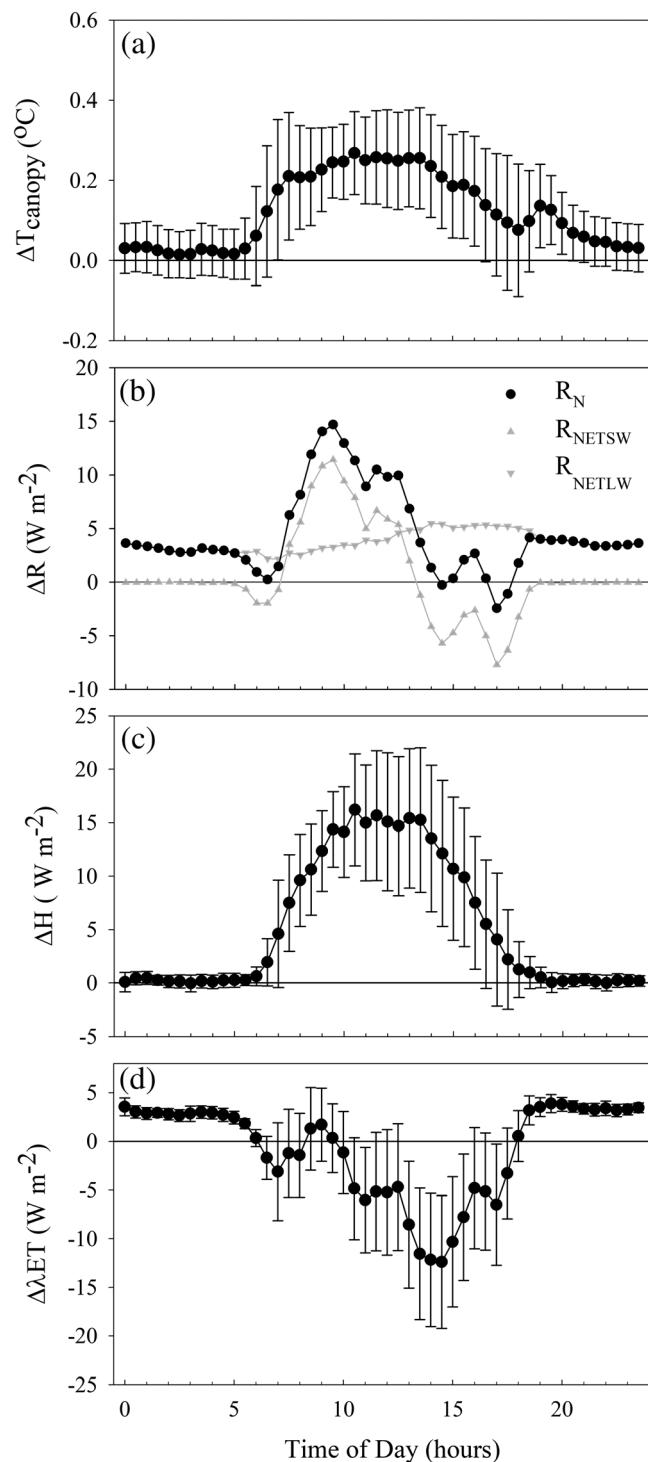


FIGURE 8 The average diurnal course of the absolute differences in energy flux between maize monoculture and alternate-row maize and soybean intercrop. (a) Canopy surface temperature (T_{canopy}), (b) net radiation (R_n), (c) sensible heat flux (H), and (d) latent heat flux (λET) are represented. Data points are equal to the intercrop minus maize monoculture per 30-min interval of the day and averaged across 52 measurement days. Negative values indicate lower values in the intercrop system, and positive values indicate higher values in the intercrop system. Error bars and replicates are as in Figure 3, excluding R_n , which was not replicated among blocks

or biological relevant ($<2 \text{ mm season}^{-1}$) despite differences in diel latent heat flux, and ultimately, the increase in grain yield per unit area by the intercrop was not sufficient to establish an increase in seasonal WUE.

The additive design of the intercrop system supports the increases in LAI and ϵ_i , while the physiological and structural dominance of maize shaped the decreases in soybean performance. An additive design denotes that the intercrop system has a higher plant density per unit area than each monoculture system of component species (Figure 1). In addition, soybean has a higher spatial clustering of leaves (leaf area density) than maize and inherently has a higher LAI in monoculture under normal growing conditions (Figure 4a). The addition of soybean between maize rows would increase leaf area per unit ground area and light interception compared to maize monoculture, which this study confirmed (Figure 4). However, the maize rows shaded 80%–90% of incident light for soybean in the intercrop system at canopy closure (Figure 3), and the performance of soybean was diminished. Intercropped soybean displayed photosynthetic shade responses (Table 1 and Figure 5, Givnish, 1988), which intensified throughout development as the structural (tall stature) and functional (C photosynthesis) dominance of maize progressed. Ultimately, soybean grain yield decreased by 94%, while the photosynthetic performance and grain yield of maize was unchanged (Tables 1 and 3 and Figures 5 and 6).

The average diel energy fluxes and canopy temperature across the season showed non-significant absolute differences between the intercrop and maize monoculture, except for latent heat flux (λET ; Figure 8). The intercrop had higher λET fluxes at night and lower λET fluxes during the day due to more energy partitioned to sensible heat flux as the intercrop canopy surface temperature was approximately $.25^\circ\text{C}$ warmer (Figure 8). However, the integration of λET over the season showed a statistically non-significant decrease in water-use ($<2 \text{ mm season}^{-1}$) by the intercrop compared to the maize monoculture (Table 2), suggesting that the diel differences in λET fluxes by the intercrop were not adequate to change seasonal water-use.

Conflicting results have been published on the water-use of intercropping systems. Previous research has shown that intercropping used less water than monocultures and produced equal or greater yields, which was concluded to arise from the higher plant density of additive designs and complementary root distributions in both spatial and temporal dimensions (Mao et al., 2012; Yang et al., 2011). In contrast, other studies showed a water-use disadvantage by a lack of complementarity for water-use (Szumigalski & Acker, 2008; Zhang et al., 2019) and by intensified interspecific competition under water stress (Wang et al., 2015). This study showed that even though additive intercrop designs have more conduits linking soil water to the atmospheric water vapor demand, if the subordinate species is heavily outcompeted, the bioenergetics of the intercrop canopy behaves similarly to the monoculture canopy of the dominant species, and a biologically relevant decrease in water-use is not achievable. Thus, gains in water-use efficiency may only be realized if interspecific competition is reduced.

TABLE 2 Seasonal water-use and water-use efficiency (WUE)

Cropping system	Measurement days	Σ ET (mm season ⁻¹)	WUE (grain yield/ Σ ET)
I _{maize/soybean}	52	284.37a \pm 7.85	4.24a \pm .30
M _{maize}	52	286.10a \pm 3.09	3.98a \pm .31
M _{soybean}	52	307.86b \pm .83	.79b \pm .03

Values represent the mean (\pm SE) of three replicate blocks ($n = 3$) with two subsamples. Letters indicate significant differences at $\alpha = 0.1$.

TABLE 3 Grain yield and land-use efficiency (LER)

Species	Cropping system	Grain yield (g m ⁻²)	Relative yield	LER
Maize	Intercrop	1180.23a \pm 81.49	1.05 \pm .06	1.11 \pm .06
	Monoculture	1131.77a \pm 78.14		
Soybean	Intercrop	13.93a \pm 1.77	.06 \pm .01	
	Monoculture	240.00b \pm 30.43		

Note: Values represent the mean (\pm SE) of three replicate blocks ($n = 3$) each with two subsamples. Relative yield and LER was calculated using Equation (7). Letters indicate significant differences within species at $\alpha = 0.1$.

Other potential ecosystem services of the maize and soybean intercrop system explored in this study must be considered in future research. If soybean were to be used as a cover crop, the living mulch may not be adequate for water savings but may be beneficial regarding weed suppression and could provide forage for grazing livestock; the protein content of soybean has been shown to increase under shade conditions (Proulx & Naeve, 2009). Measuring the energy fluxes, including soil heat flux, under drought conditions and at larger scales must also be considered to determine whether small water savings matters to farmers. Efforts to partition λ ET within the intercrop system would also refine the relative contributions of each component crop to whole system water-use (Ma et al., 2020).

5 | CONCLUSION

The additive and simultaneous alternate-row maize/soybean intercrop system established marginal increases in (1) light interception efficiency compared to the standard maize monoculture of the U.S. Corn Belt due to a higher amount of leaf area per unit ground area at canopy closure and (2) land-use efficiency since the photosynthetic performance and grain yield of maize was unaffected by intercropping. However, seasonal water-use under rainfed conditions was similar to the standard maize monoculture and the increase in water-use efficiency by the intercrop was statistically insignificant, however, what would constitute a biologically relevant effect is unknown(?). This was likely due to the competitive advantage of maize dominating the intercrop canopy over soybean and thereby translating canopy bioenergetics close to that of the maize monoculture canopy. While there were no statistical or biological relevant differences in maize productivity and whole system water-use, intercropping high-performing crop cultivars in a dense configuration without much negative impact suggests that efforts to increase yield and water-use efficiency may lead to improved benefits.

ACKNOWLEDGMENTS

This work was funded by the USDA to the Global Change and Photosynthesis Research Unit of the USDA Agricultural Research Service. Mention of trade names or commercial products in this publication is solely to provide specific information and does not imply recommendation or endorsement by the U.S. Department of Agriculture. USDA is an equal opportunity provider and employer. Any opinions, findings, and conclusions or recommendations expressed in this publication are those of the author(s) and do not necessarily reflect the views of the U.S. Department of Agriculture. The authors thank Tim Mies, David Drag, Ben Harbaugh, Ben Thompson, and Trace Elliot for their management and assistance of the Energy Farm Facility and preparations of the field for this project. The authors also thank Taylor Pederson, David Drag, Evan Dracup, Caitlin Moore, Emily Timm, Marshall Mitchell and Pietro Hughes for their assistance with data collection and sensor maintenance.

CONFLICT OF INTEREST

Authors declare no conflict of interest.

ORCID

Elena A. Pelech  <https://orcid.org/0000-0001-5084-324X>

Brendan C. S. Alexander  <https://orcid.org/0000-0001-5566-0469>

Carl J. Bernacchi  <https://orcid.org/0000-0002-2397-425X>

REFERENCES

- Arshad, M. (2021). Fortnightly dynamics and relationship of growth, dry matter partition and productivity of maize based sole and intercropping systems at different elevations. *European Journal of Agronomy*, 130, 126377. <https://doi.org/10.1016/j.eja.2021.126377>
- Arshad, M., Nawaz, R., Ahmad, S., Razaq, A., Ranamukhaarachchi, S. L., & Rahman, S. (2020). Relative production efficiency of maize-legume Intercroppings at different altitudes. *Journal of the National Science Foundation of Sri Lanka*, 48, 409–420. <https://doi.org/10.4038/jnsfr.v48i4.8803>



- Baker, N. R. (2008). Chlorophyll fluorescence: A probe of photosynthesis in vivo. *Annual Review of Plant Biology*, 59, 89–113. <https://doi.org/10.1146/annurev-arplant.59.032607.092759>
- Baldocchi, D. D., Hincks, B. B., & Meyers, T. P. (1988). Measuring biosphere-atmosphere exchanges of biologically related gases with micrometeorological methods. *Ecology*, 69, 1331–1340. <https://doi.org/10.2307/1941631>
- Bellasio, C., Beerling, D. J., & Griffiths, H. (2015). An excel tool for deriving key photosynthetic parameters from combined gas exchange and chlorophyll fluorescence: Theory and practice. *Plant, Cell & Environment*, 39, 1180–1197. <https://doi.org/10.1111/pce.12560>
- Bellasio, C., Beerling, D. J., & Griffiths, H. (2016). Deriving C4 photosynthetic parameters from combined gas exchange and chlorophyll fluorescence using an excel tool: Theory and practice. *Plant, Cell & Environment*, 39, 1164–1179. <https://doi.org/10.1111/pce.12626>
- Bernacchi, C. J., & VanLoocke, A. (2014). Terrestrial ecosystems in a changing environment: A dominant role for water. *Annual Review of Plant Biology*, 66, 1–24. <https://doi.org/10.1146/annurev-arplant-043014-114834>
- Bernacchi, C. J., Kimball, B. A., Quarles, D. R., Long, S. P., & Ort, D. R. (2007). Decreases in stomatal conductance of soybean under open-air elevation of [CO₂] are closely coupled with decreases in ecosystem evapotranspiration. *Plant Physiology*, 143, 134–144. <https://doi.org/10.1104/pp.106.089557>
- Brooker, R. W., Bennett, A. E., Cong, W., Daniell, T. J., George, T. S., Hallett, P. D., Hawes, C., Iannetta, P. P. M., Jones, H. G., Karley, A. J., Li, L., McKenzie, B. M., Pakeman, R. J., Paterson, E., Schöb, C., Shen, J., Squire, G., Watson, C. A., Zhang, C., ... White, P. J. (2015). Improving intercropping: A synthesis of research in agronomy, plant physiology and ecology. *The New Phytologist*, 206, 107–117. <https://doi.org/10.1111/nph.13132>
- Cardinale, B. J., Wright, J. P., Cadotte, M. W., Carroll, I. T., Hector, A., Srivastava, D. S., Loreau, M., & Weis, J. J. (2007). Impacts of plant diversity on biomass production increase through time because of species complementarity. *Proceedings of the National Academy of Sciences of the United States of America*, 104, 18123–18128. <https://doi.org/10.1073/pnas.0709069104>
- Condon, A. G., Richards, R. A., Rebetzke, G. J., & Farquhar, G. D. (2002). Improving intrinsic water-use efficiency and crop yield. *Crop Science*, 42, 122–131. <https://doi.org/10.2135/cropsci2002.1220>
- DeLucia, E. H., Chen, S., Guan, K., Peng, B., Li, Y., Gomez-Casanovas, N., Kantola, I. B., Bernacchi, C. J., Huang, Y., Long, S. P., & Ort, D. R. (2019). Are we approaching a water ceiling to maize yields in the United States? *Ecosphere*, 10, e02773. <https://doi.org/10.1002/ecs2.2773>
- Ficklin, D. L., & Novick, K. A. (2017). Historic and projected changes in vapor pressure deficit suggest a continental-scale drying of the United States atmosphere. *Journal of Geophysical Research-Atmospheres*, 122, 2061–2079. <https://doi.org/10.1002/2016jd025855>
- Givnish, T. (1988). Adaptation to Sun and shade: A whole-plant perspective. *Functional Plant Biology*, 15, 63–92. <https://doi.org/10.1071/pp9880063>
- Jackson, R. D., Moran, M. S., Gay, L. W., & Raymond, L. H. (1987). Evaluating evaporation from field crops using airborne radiometry and ground-based meteorological data. *Irrigation Science*, 8, 81–90. <https://doi.org/10.1007/bf00259473>
- Kimball, B. A., LaMorte, R. L., Pinter, P. J., Wall, G. W., Hunsaker, D. J., Adamsen, F. J., Leavitt, S. W., Thompson, T. L., Matthias, A. D., & Brooks, T. J. (1999). Free-air CO₂ enrichment and soil nitrogen effects on energy balance and evapotranspiration of wheat. *Water Resources Research*, 35, 1179–1190. <https://doi.org/10.1029/1998wr900115>
- Lawson, T., & Blatt, M. R. (2014). Stomatal size, speed, and responsiveness impact on photosynthesis and water use efficiency. *Plant Physiology*, 164, 1556–1570. <https://doi.org/10.1104/pp.114.237107>
- Lenth, R. V. (2021). Emmeans: Estimated marginal means, aka least-squares means. R Package Version 1.6.2-1. <https://CRAN.R-project.org/package=emmeans>
- Li, C., Hoffland, E., Kuyper, T. W., Yu, Y., Zhang, C., Li, H., Zhang, F., & van der Werf, W. (2020). Syndromes of production in intercropping impact yield gains. *Nat Plants*, 1–8, 653–660. <https://doi.org/10.1038/s41477-020-0680-9>
- Lobell, D. B., Cassman, K. G., & Field, C. B. (2009). Crop yield gaps: Their importance, magnitudes, and causes. *Annual Review of Environment and Resources*, 34, 179–204. <https://doi.org/10.1146/annurev-environ.041008.093740>
- Long, S. P., & Bernacchi, C. J. (2003). Gas exchange measurements, what can they tell us about the underlying limitations to photosynthesis? Procedures and sources of error. *Journal of Experimental Botany*, 54, 2393–2401. <https://doi.org/10.1093/jxb/erg262>
- Ma, L., Li, Y., Wu, P., Zhao, X., Chen, X., & Gao, X. (2020). Coupling evapotranspiration partitioning with water migration to identify the water consumption characteristics of wheat and maize in an intercropping system. *Agricultural and Forest Meteorology*, 290, 108034. <https://doi.org/10.1016/j.agrformet.2020.108034>
- Mao, L., Zhang, L., Li, W., van der Werf, W., Sun, J., Spiertz, H., & Li, L. (2012). Yield advantage and water saving in maize/pea intercrop. *Field Crops Research*, 138, 11–20. <https://doi.org/10.1016/j.fcr.2012.09.019>
- Meyers, T. P., & Hollinger, S. E. (2004). An assessment of storage terms in the surface energy balance of maize and soybean. *Agricultural and Forest Meteorology*, 125, 105–115. <https://doi.org/10.1016/j.agrformet.2004.03.001>
- Morris, R. A., & Garrity, D. P. (1993). Resource capture and utilization in intercropping: Water. *Field Crops Research*, 34, 303–317. [https://doi.org/10.1016/0378-4290\(93\)90119-8](https://doi.org/10.1016/0378-4290(93)90119-8)
- Ort, D. R., & Long, S. P. (2014). Limits on yields in the Corn Belt. *Science*, 344, 484–485. <https://doi.org/10.1126/science.1253884>
- Pinheiro, J., Bates, D., DebRoy, S., & Sarkar, D., & R Core Team. (2021). Nlme: Linear and nonlinear mixed effects models. R Package Version 3.1–152. <https://CRAN.R-project.org/package=nlme>
- Proulx, R. A., & Naeve, S. L. (2009). Pod removal, shade, and defoliation effects on soybean yield, protein, and oil. *Agronomy Journal*, 101, 971–978. <https://doi.org/10.2134/agnonj2008.0222x>
- R Core Team. (2021). R: A language and environment for statistical computing. R Foundation for Statistical Computing, Vienna, Austria. <http://www.R-project.org/>
- Soil Survey Staff. (2015). Natural Resources Conservation Service, United States Department of Agriculture. Official Soil Series Descriptions. Retrieved from https://www.nrcs.usda.gov/wps/portal/nrcs/detail/soils/scientists/?cid=nrcs142p2_053587
- Szumigalski, A. R., & Acker, R. C. V. (2008). Land equivalent ratios, light interception, and water use in annual intercrops in the presence or absence of in-crop herbicides. *Agronomy Journal*, 100, 1145–1154. <https://doi.org/10.2134/agnonj2006.0343>
- Tilman, D., Balzer, C., Hill, J., & Befort, B. L. (2011). Global food demand and the sustainable intensification of agriculture. *Proceedings of the National Academy of Sciences*, 108, 20260–20264. <https://doi.org/10.1073/pnas.1116437108>
- Triggs, J. M., Kimball, B. A., Pinter, P. J., Wall, G. W., Conley, M. M., Brooks, T. J., LaMorte, R. L., Adam, N. R., Ottman, M. J., Matthias, A. D., Leavitt, S. W., & Cerveny, R. S. (2004). Free-air CO₂ enrichment effects on the energy balance and evapotranspiration of sorghum. *Agricultural and Forest Meteorology*, 124, 63–79. <https://doi.org/10.1016/j.agrformet.2004.01.005>
- Vandermeer, J. H. (1989). *The ecology of intercropping*. Cambridge University Press. <https://doi.org/10.1017/CBO9780511623523>

- Wang, Z., Zhao, X., Wu, P., & Chen, X. (2015). Effects of water limitation on yield advantage and water use in wheat (*Triticum aestivum* L.)/maize (*Zea mays* L.) strip intercropping. *European Journal of Agronomy*, 71, 149–159. <https://doi.org/10.1016/j.eja.2015.09.007>
- Yang, C., Huang, G., Chai, Q., & Luo, Z. (2011). Water use and yield of wheat/maize intercropping under alternate irrigation in the oasis field of Northwest China. *Field Crops Research*, 124, 426–432. <https://doi.org/10.1016/j.fcr.2011.07.013>
- Zhang, Y., Duan, Y., Nie, J., Yang, J., Ren, J., van der Werf, W., Evers, J. B., Zhang, J., Su, Z., & Zhang, L. (2019). A lack of complementarity for water acquisition limits yield advantage of oats/vetch intercropping in a semi-arid condition. *Agricultural Water Management*, 225, 105778. <https://doi.org/10.1016/j.agwat.2019.105778>

SUPPORTING INFORMATION

Additional supporting information may be found in the online version of the article at the publisher's website.

How to cite this article: Pelech, E. A., Alexander, B. C. S., & Bernacchi, C. J. (2021). Photosynthesis, yield, energy balance, and water-use of intercropped maize and soybean. *Plant Direct*, 5(12), e365. <https://doi.org/10.1002/pld3.365>